Journal of Cell Science 109, 2319-2329 (1996)
Printed in Great Britain © The Company of Biologists Limited 1996
JCS8018

Alterations in neural intermediate filament organization: functional implications and the induction of pathological changes related to motor neuron disease

Karen Straube-West[1,*], Patricia A. Loomis[2,*], Puneet Opal[3] and Robert D. Goldman[2,†]

[1]Department of Pharmacology, SUNY, 750 East Adams Street, Syracuse, NY 13210, USA
[2]Department of Cell and Molecular Biology, Northwestern University Medical School, 303 East Chicago Avenue, Chicago, IL 60611, USA
[3]Department of Neurology, University of Iowa, Iowa City, IA 52242, USA

*These authors contributed equally to this work
†Author for correspondence

SUMMARY

The properties regulating the supramolecular organization of neural intermediate filament (NIF) networks have been investigated in cultured dorsal root ganglion (DRG) neurons. The studies described take advantage of the ability of endogenous NIF to incorporate purified biotinylated neurofilament triplet (NFT) proteins, NF-L, NF-M and NF-H. When injected at concentrations of 0.8-1.0 mg/ml injection buffer, each of these proteins is incorporated without perturbing the endogenous NIF network. However, at progressively higher concentrations, NF-H induces the aggregation and accumulation of NIF in the cell body. Subsequent to the induction of these aggregates, numerous alterations in the cytoarchitecture of neurons can be detected. The latter occur in a temporal sequence which appears to begin with the fragmentation of the Golgi complex. At later times, accumulation of mitochondria within the proximal region of neurites, peripheralization of the nucleus, and a significant decrease in neurite caliber become obvious. After longer time periods, the NIF aggregates are seen to react with an antibody which reveals abnormally phosphorylated NF-H. These observations demonstrate that an imbalance in the normal stoichiometric relationships among the NFT proteins rapidly alters the supramolecular organization of the NIF network. These changes most likely reflect the normal functions of neurofilaments in cell shape and the organization and cytoplasmic distribution of membranous organelles. Interestingly, virtually all of these changes closely resemble those which have been reported in motor neuron diseases such as amyotrophic lateral sclerosis (ALS). These findings suggest that cultured neurons can be used as models for more precisely defining the relationships between the formation of NIF aggregates and the sequence of cytopathological events which typify neurodegenerative diseases.

Key words: Neurofilament, Amyotrophic lateral sclerosis, Golgi complex, Intermediate filament

INTRODUCTION

Neural intermediate filaments (NIF) containing one or more of five different types of subunit proteins have been identified (see Nixon and Shea, 1992). The majority of adult neurons express Type IV intermediate filaments (IF), also known as the triplet proteins NF-L (~68 kDa), NF-M (~95 kDa) and NF-H (~110 kDa; Bennett et al., 1981, 1984; Hoffman and Lasek, 1975; Liem et al., 1978). As in all IF, NIF possess common structural features, including a conserved alpha-helical central rod domain, flanked by less-well conserved amino- and carboxy-terminal domains (see Steinert and Roop, 1988). In vitro NF-L is capable of forming IF, while NF-M and NF-H cannot (Geisler and Weber, 1981; Liem and Hutchison, 1982; Gardner et al., 1984). However, NF-M and NF-H can each participate in the formation of NIF in the presence of NF-L (Zackroff et al., 1982; Hisanaga and Hirokawa, 1988; Balin and Lee, 1991). In vivo, NF-L cannot form an NIF network, however, it can do so in the presence of NF-M and/or NF-H suggesting that NIF are obligate heteropolymers (Ching and Liem, 1993; Lee et al., 1993).

It has been demonstrated that IF networks in general are in a state of dynamic equilibrium, resulting in the continuous exchange of proteins between subunit and polymerized forms in growing cells in culture (Vikstrom et al., 1989, 1992; Miller et al., 1993). With respect to NIF in particular, the data derived from fluorescence energy transfer, fluorescence recovery after photobleaching (FRAP) and transient transfection experiments, suggest that there is an exchange between polymerized NIF and a 'soluble' pool in vitro (Angelides et al., 1989) and in vivo (Okabe et al., 1983; Takeda et al., 1994; Ching and Liem, 1993).

Although little is known about specific NIF functions, positive correlations exist between NIF number and axon

caliber (Friede and Samorajski, 1970; Weiss and Mayr, 1971). In regenerating nerve fibers, NFT gene expression is depressed and there is a reduction in axon caliber and the number of NIF (Hoffman et al., 1984, 1985). A deficiency of NIF in the mutant quail (*quv*), has been correlated with a reduction in the radial growth of axons (Yamasaki et al., 1992; Ohara et al., 1993). Taken together, these observations suggest that it is the number of NIF which regulates axon caliber. However, in transgenic mice which overexpress only NF-L, there is an increase in the number of NIF without a concurrent effect on axonal caliber (Monteiro et al., 1990). The latter discrepancy may be explained in part by the finding that the expression of NF-H follows that of NF-L and NF-M during development (Shaw and Weber, 1982; Willard and Simon, 1983), and that NF-H expression coincides with a period of increasing radial growth of axons (Willard and Simon, 1983; Hoffman et al., 1984, 1985). In this regard, it is thought that the long carboxy-tails of NF-H and NF-M project from NIF (Hisanaga and Hirokawa, 1988), and thereby modulate NIF spacing (see Shaw, 1991; Nakagawa et al., 1995). In turn, the configuration of the NF-H tail domain appears to be regulated by phosphorylation (Sternberger and Sternberger, 1983; Hoffman et al., 1985; Carden et al., 1985; deWaegh et al., 1992; Nixon, 1993). From a functional point of view, axon caliber has been related to important neurophysiological activities, including conduction velocity (Gasser and Grundfest, 1939), the order of recruitment of fibers during development (Henneman et al., 1965), and the establishment of the myelin sheath in the large diameter neurons of the peripheral nervous system (Voyvodic, 1989).

Transgenic mice which express 1.5-2.0 times the normal level of the human NF-H gene, display abnormal aggregates of NIF in the cell bodies of motor neurons, and subsequently the appearance of motor neuron disease (ALS)-like symptoms (Carpenter, 1968; Collard et al., 1995; Côté et al., 1993; Hirano et al., 1984). NF-L and NF-M overexpression also result in accumulations of NIF in the motor neurons of transgenic mice (Xu et al., 1993; Vickers et al., 1994). Mice expressing low levels of mutant NF-L also display NIF aggregation and motor neuron pathology (Lee et al., 1994). Collectively, these studies show that alterations in either the subunit ratios of the NFT proteins or inhibition of their assembly properties have important consequences for the physiological and morphological properties of neurons.

Although studies of transgenic mice have linked changes in the supramolecular organization of NIF to neurodegenerative disease, it is difficult to use animals to study the temporal relationships between the formation of neurofilament aggregates and the numerous structural and physiological changes which take place in single neurons. This is due to the fact that whole animal studies require relatively long time periods ranging from days to months and involve primarily post-mortem preparations of nervous tissue. In this study, we use single cells to more precisely define the dynamic properties and functions of NIF, as well as their relationships to neurodegeneration. This single cell method involves the microinjection of solutions of NFT proteins into cultured dorsal root ganglion neurons. The results demonstrate that these neurons can incorporate exogenous NFT subunits into their endogenous NIF post-translationally. We have also examined the consequences of significantly altering the balance amongst the triplet proteins by microinjecting increasing amounts of NF-H. The data obtained demonstrate that we can induce alterations in the supramolecular organization of endogenous NIF which trigger a cascade of structural alterations resulting in neurons which appear similar to those seen in diseased motor neurons of ALS patients.

MATERIALS AND METHODS

Cell culture

Dorsal root ganglia (DRGs) were dissected from E14-17 chicken embryos as described by Hamburger and Hamilton (1951), rinsed in PBSa, and then incubated in 0.2 mg/ml collagenase/dispase (Boehringer Mannheim, Indianapolis, IN), 0.2 mg/ml papain (Boehringer Mannheim), and 0.5 mg/ml L-cysteine (Sigma, St Louis, MO) in PBSa for 15 minutes at 37°C (Arakawa et al., 1992). Digestion was terminated by adding 1 mg/ml fetal bovine serum (Gibco, Grand Island, NY) and cells were plated at a density of 10^5/ml onto either plain or locator coverslips (Bellco, Vineland, NJ) coated with laminin (Sigma). Cells were maintained in a 37°C incubator with 10% CO_2 in Ham's F-12 medium containing 10% fetal calf serum (Gibco), 1% penicillin/streptomycin, 25 ng/ml nerve growth factor (Sigma) and 5 μM cytosine arabinoside. Live cells were observed with differential interference contrast (DIC) optics before and following microinjection. Before an experiment, coverslips were sealed to the bottom of 35 mm culture dishes with paraffin to cover holes made in the bottom of the dishes. The dishes were filled with the appropriate medium and incubated at 37°C for 1 hour prior to observation.

Preparation of biotinylated NFT proteins

Bovine spinal cord NIF-enriched fractions were prepared using slight modifications of published procedures (Zackroff et al., 1982; Geisler and Weber, 1981; Hisanaga and Hirokawa, 1988). Spinal cords were homogenized in a Waring blender in 1.4 ml of Buffer H (100 mM Pipes, pH 6.8, 5 mM EGTA, 1 mM $MgCl_2$, 1 mM PMSF) per gram of tissue, and the homogenate was centrifuged (28,000 ***g*** for 50 minutes at 4°C). Glycerol was added to the supernatant (20:80, v/v), and it was incubated at 37°C for 90 minutes, followed by centrifugation at 150,000 ***g*** for 90 minutes (4°C). The resulting pellet, enriched in NIF, was dissolved in extraction buffer (10 mM sodium phosphate, pH 7.5, 1 mM EGTA, 6 M urea, 0.5 mM DTT, 1 mM PMSF and 5 μg/ml each of aprotinin, leupeptin and pepstatin; Sigma), at a final protein concentration of 2-3 mg/ml. Aliquots were subsequently dialyzed for 2 hours (37°C) against assembly buffer (50 mM MES, pH 6.25, 1 mM DTT, 175 mM NaCl, 0.5 mM EGTA; Aebi et al., 1988), followed by dialysis against the same buffer at pH 7.0 for 1 hour, prior to biotinylation with *N*-hydroxysuccinimidobiotin (Molecular Probes, Eugene, OR) according to the method of Vikstrom et al. (1990).

Polymerized biotinylated NIF were centrifuged at 200,000 ***g*** and the pellets were washed with assembly buffer to remove excess biotin cross-linking reagent. The pellets were dissolved in extraction buffer at a protein concentration of 7 mg/ml, and the NFTs were purified by ion exchange chromatography using DEAE cellulose and a 65-250 mM NaCl gradient to purify NF-H. Further separation was achieved by loading the impure fractions onto a second DEAE-cellulose column and eluting with an 8-0 M urea gradient (Geisler and Weber, 1981; Zackroff et al., 1982; Hisanaga and Hirokawa, 1988). Fractions rich in NF-H, NF-M and NF-L were identified by SDS-PAGE, pooled separately, dialyzed against 50 mM ammonium bicarbonate and concentrated by lyophilization. Subsequently, these fractions were dissolved in extraction buffer and dialyzed against microinjection buffer. Aliquots were stored at −70°C until needed.

The frozen aliquots of biotinylated NFT proteins were tested for their ability to form IF in vitro prior to microinjection. Samples were dialyzed against assembly buffer, applied to a carbon/parlodion coated electron microscope grid, and negatively stained with aqueous

1% uranyl acetate. These preparations were examined with a JEOL 1200CX electron microscope.

In some experiments, NF-H was dephosphorylated prior to microinjection by treatment with 1 unit of alkaline phosphatase (Boehringer Mannheim) per mg of protein for 2 hours at 37°C. The phosphatase was inactivated by freezing and the sample was concentrated and dialyzed into microinjection buffer (5 mM sodium phosphate, pH 8.0, 0.2% 2-mercaptoethanol).

Microinjection

Frozen aliquots of each triplet protein were thawed and clarified by centrifugation in an Eppendorf microfuge prior to microinjection. Protein concentrations were determined by the method of Bradford (1976). Where required, biotinylated NF-H was concentrated using Microcon-30 tubes (Amicon, Beverly, MA). For control studies, bovine serum albumin (BSA; Pierce Chemical Company, Rockford, IL) was biotinylated, dialyzed into microinjection buffer and stored at −20°C until needed. The proteins were microinjected (Vikstrom et al., 1989, 1990) into the cell bodies of chick or mouse DRG neurons which had been cultured for 24-72 hours.

Microscopy

Neurons cultured on locator coverslips were microinjected, placed in a 37°C incubator and at time intervals were rinsed in PBSa and fixed for indirect immunofluorescence in methanol (−20°C) as previously described (Yang et al., 1985). All antibodies were diluted 1:20 in PBSa. In some preparations, fixed neurons were incubated in 10% normal donkey serum, and then processed for double label immunofluorescence with goat anti-biotin (Sigma) and a mouse monoclonal anti-NF-L (Amersham, Arlington Heights, IL) for 30 minutes at 37°C. In other experiments similar procedures were used with several different antibodies including a phosphoepitope-specific antibody directed against mouse NF-H (RMO24, a gift from Dr Virginia Lee of the University of Pennsylvania; Lee et al., 1987), a rabbit antibody against bovine NIF, a rabbit antibody directed against HSP60 (Stressgen Biotechnologies, Victoria, BC) for staining mitochondria, a mouse monoclonal antibody directed against the Golgi 58K protein (Sigma), and a rabbit antibody directed against tubulin (a gift from Dr Chloe Bulinsky of Columbia University). After incubation in primary antibodies, coverslips were washed with 3 changes of PBSa over 15 minutes and were subsequently incubated with the appropriate secondary antibodies. These included donkey anti-goat and anti-mouse IgG conjugated with fluorescein, and donkey anti-mouse IgG conjugated with rhodamine (Jackson Immunoresearch, West Grove, PA), for 30 minutes at 37°C. Coverslips were washed again in PBSa and mounted on glass slides in gelvatol containing 100 mg/ml Dabco (1,4-diazabicyclo[2.2.2.]octane; Aldrich Chemical Co.). Cells were examined with a Zeiss Laser Scan Microscope (LSM) equipped with a 488λ argon laser and a 543λ helium-neon laser. Some non-confocal images were obtained with the Image-1 system (Universal Imaging Corp., West Chester, PA). These images, as well as all confocal images, were printed with a Sony UP-8000 video printer.

Live cell observations were made on a Nikon inverted microscope using a ×40 objective equipped with DIC optics. Images of each cell were obtained using a DAGE nuvicon camera interfaced with either a Hamamatsu Argus-10 or the Image-1 system and stored on optical disks. Images of the same cell before and 24 hours following microinjection were obtained and stored for later comparison. Measurements of neurite width were made on each cell using the Image-1 caliper function and the data were analyzed statistically using Excel spreadsheet software (Microsoft Corporation, Redmond, WA).

SDS-PAGE and immunoblotting

Purified NFT proteins and/or biotinylated proteins were separated on 8.0% polyacrylamide gels according to the method of Laemmli (1970). The separated proteins were transferred to nitrocellulose (Towbin et al., 1979) and probed with either goat anti-biotin (Sigma), or mouse monoclonal antibodies against NF-L, NF-M, and NF-H (Amersham). The antibodies were diluted in 5% non-fat dry milk in PBSa at a concentration of 1:500 for all primary and 1:1,000 for all secondary antibodies. The latter included donkey anti-goat and donkey anti-mouse horseradish peroxidase conjugates (Amersham). All secondary antibodies were purchased from Amersham.

RESULTS

In vitro characterization of biotinylated NIF proteins

Bovine spinal cord NIF were prepared, biotinylated, and purified as described in Materials and Methods. Fractions containing biotinylated NF-L, NF-M and NF-H were pooled, assayed by SDS-PAGE and transferred to nitrocellulose for immunoblotting. Each fraction was shown to consist of one

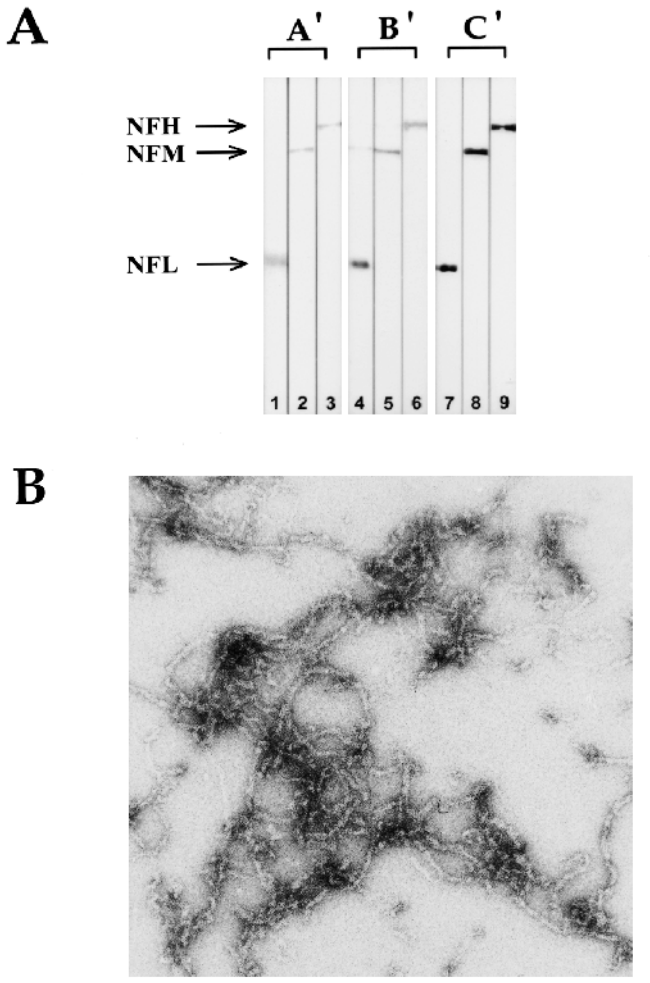

Fig. 1. Characterization of biotinylated NFT proteins. (A) Following biotinylation and separation by column chromatography, the fractions corresponding to each of the three NIF proteins were pooled, subjected to SDS-PAGE, transferred to nitrocellulose and stained with either amino black (A′, lanes 1-3), or immunoblotted with anti-biotin antibody (B′, lanes 4-6) or mouse monoclonal antibodies directed against each of the NIF triplet proteins (C′, lane 7, anti-NF-L; lane 8, anti-NF-M; lane 9, anti-NF-H). (B) Negative stain electron micrograph of NIF reassembled from purified biotinylated NFT proteins. ×49,000.

major band of the correct molecular mass (Fig. 1A). Each of these purified proteins reacted with anti-biotin and the appropriate NFT antibody, as determined by immunoblotting (Fig. 1A). When mixed in equal amounts by weight, the purified biotinylated NFT proteins formed NIF which appeared similar in morphology to those reported by other investigators (Geisler and Weber, 1981; Liem and Hutchison, 1982; Gardner et al., 1984; Fig. 1B). Biotinylated NF-M and NF-H alone did not form NIF in agreement with previously published results (Geisler and Weber, 1981; Liem and Hutchison, 1982; Zackroff et al., 1982; Gardner et al., 1984), and NF-L alone could form only very short filaments (data not shown; Zackroff et al., 1982; Hisanaga and Hirokawa, 1988; Balin and Lee, 1991).

The incorporation of microinjected NFT proteins into the endogenous NIF network

Both chick and mouse embryonic DRG neurons were used in our studies and the results were essentially identical. However, only chick neurons are discussed as the cell bodies are larger, making it easier to carry out the microinjection experiments and to resolve the details of the endogenous NIF networks. At concentrations of 0.8-1.0 mg/ml, biotinylated NF-H was not obviously associated with endogenous NIF when cells were observed immediately after microinjection (Fig. 2A,B). Within 30 minutes, anti-biotin revealed short filamentous structures throughout the cell body, most of which were coincident with fibrous elements of the endogenous NIF network, as shown by staining with anti-NF-L (data not shown). After 2.5-3 hours, an extensive biotinylated network was seen to be coincident with the endogenous NIF network (Fig. 2C,D).

At the same concentrations, microinjected biotinylated NF-M and NF-L displayed a pattern of incorporation which was identical to that seen for NF-H (data not shown). However, the time for incorporation was slower. For NF-M, a completely coincident biotinylated network was not seen for about 4 hours and for NF-L about 5 hours post-injection. Using these concentrations of the NFT proteins, no obvious changes were seen in the organization of the endogenous NIF network as depicted in Fig. 3E.

NF-H induces NIF aggregates following injection at higher concentrations

We also determined the in vivo effects of altering more significantly the stoichiometric relationships among the triplet proteins. We found that we could concentrate biotinylated NF-H up to 10 mg/ml and still retain it in an injectable form. This was not the case for NF-L and NF-M, which tended to aggregate and clog the injection needle at concentrations greater than 2 mg/ml. Therefore, we studied the effects of altering NF-H concentrations relative to endogenous NF-L and NF-M. We used anti-NF-L staining to monitor the organization of the endogenous NIF networks in NF-H microinjected cells. In all cases anti-biotin was used to confirm that we were only monitoring microinjected cells.

Three hours following the injection of 3 mg/ml NF-H, approximately 25% of the cells displayed thicker filamentous structures (NIF aggregates) relative to control cells (Fig. 3A,E). At 24 hours following microinjection, the same percentage of the cells contained obvious NIF aggregates (Fig. 3C). Increasing the concentration of microinjected NF-H to 5 mg/ml yielded morphologically similar results; however, NIF aggregates became apparent in approximately 50% of injected cells at earlier time points relative to those formed at lower concentrations of NF-H (Fig. 3B). At 24 hours after injection, the affected neurons contained very large masses of NIF aggregates which frequently appeared to displace the nucleus into a peripheral position (Fig. 3D).

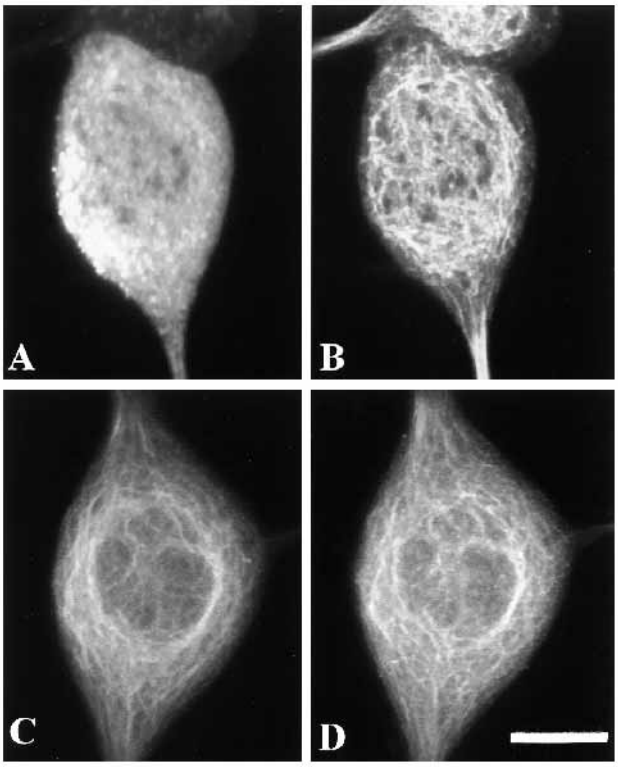

Fig. 2. Biotinylated NF-H is incorporated into endogenous NIF. Neurons were microinjected with biotinylated NF-H and fixed and stained with anti-biotin (A,C) and anti-NF-L (B,D), 15 minutes (A and B), and 3 hours (C and D) post-injection. Bar, 10 μm.

In order to confirm that our observations were the result of the addition of higher concentrations of NF-H, and not the result of a generalized response to an increase in soluble protein in the cells, we also microinjected 4-10 mg/ml of biotinylated bovine serum albumin (BSA) and fixed the cells at time intervals up to 24 hours following microinjection. Under these conditions, we were not able to observe any alterations in the organization of the NIF network (data not shown).

The induction of NIF aggregates is related to changes in the transport, localization and organization of membranous organelles

Neurons induced to form NIF aggregates following injection with 3-5 mg/ml NF-H, display alterations in the location and organization of the Golgi complex within 12 hours following microinjection (compare Fig. 4A,B with C,D). Specifically, the complex which is normally organized as long sac-like structures, frequently concentrated in the perinuclear region, was found to be fragmented into small pieces and distributed throughout the cell body (see Fig. 4D). The distribution of mitochondria was also affected and this became obvious in all

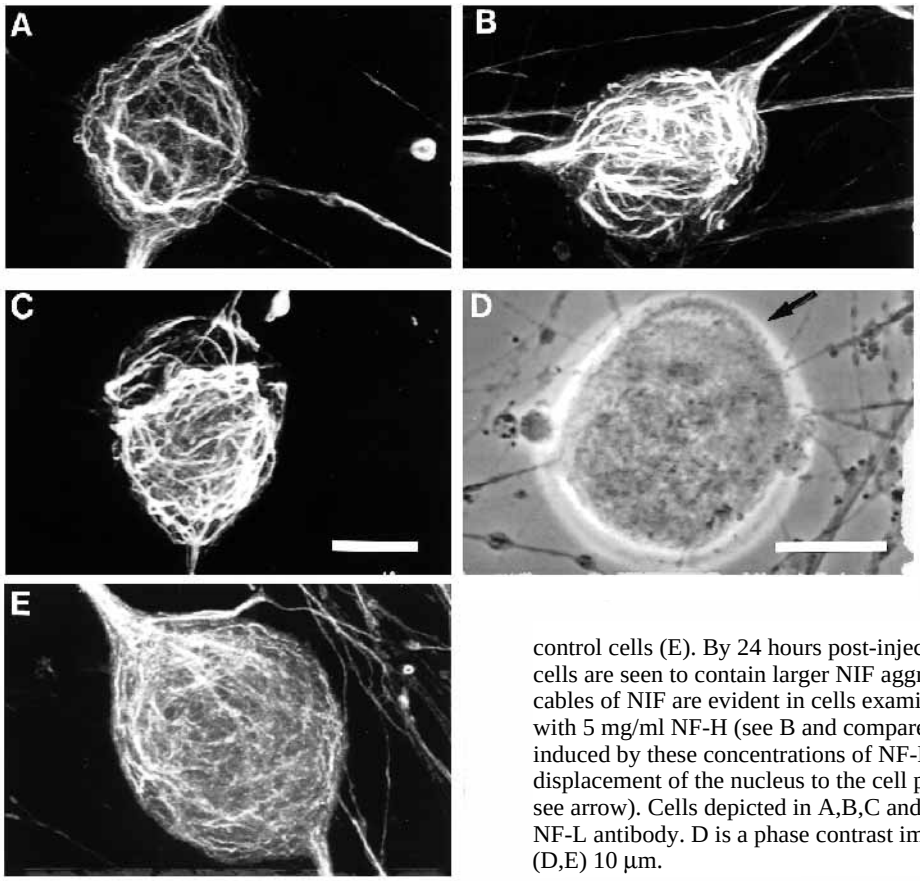

Fig. 3. Microinjection with 3-7 mg/ml NF-H results in alterations of NIF organization. At 3 hours post-injection with 3 mg/ml NF-H, the endogenous NIF network appears to contain thick filamentous structures (A) when compared to control cells (E). By 24 hours post-injection with 3 mg/ml NF-H, cells are seen to contain larger NIF aggregates (C). Even thicker cables of NIF are evident in cells examined 3 hours post-injection with 5 mg/ml NF-H (see B and compare with A). NIF aggregates induced by these concentrations of NF-H frequently cause displacement of the nucleus to the cell periphery (7 mg/ml NF-H; D, see arrow). Cells depicted in A,B,C and E were stained with anti-NF-L antibody. D is a phase contrast image. Bars: (A,B,C) 10 μm; (D,E) 10 μm.

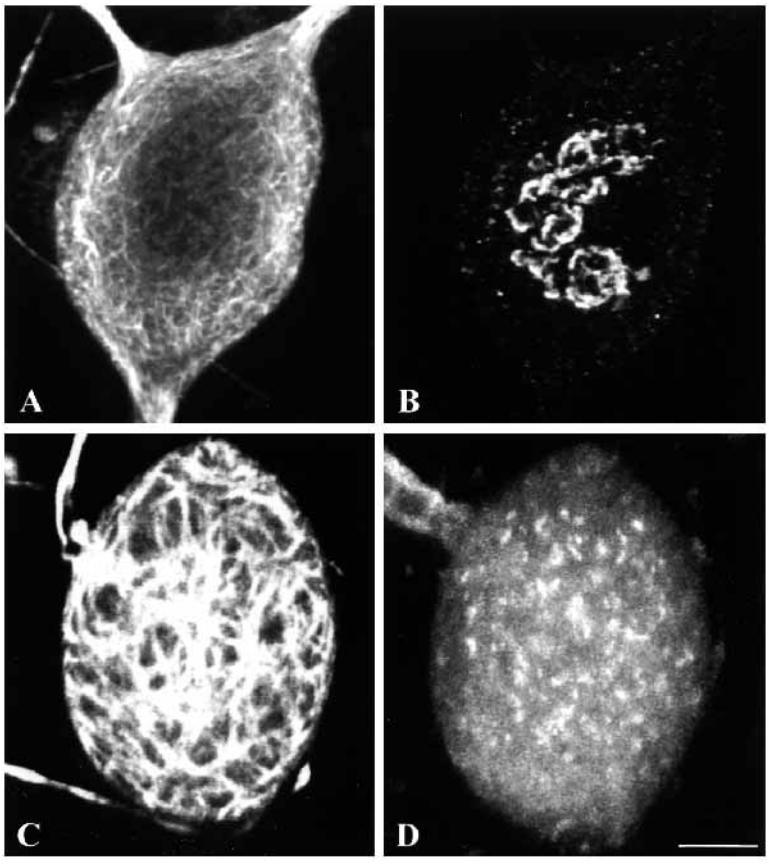

Fig. 4. Localization of the Golgi complex in NIF aggregate bearing neurons. In control cells in which there is a normal NIF network (A), the Golgi complex consists of a collection of long sac-like structures, frequently localized in the perinuclear region (B). When NIF aggregates are induced (C), the Golgi becomes fragmented into small segments which are distributed throughout the cell body (D). Double label immunofluorescence with anti-NF-L (A,C) and anti-Golgi 58K (B,D). Bar, 5 μm.

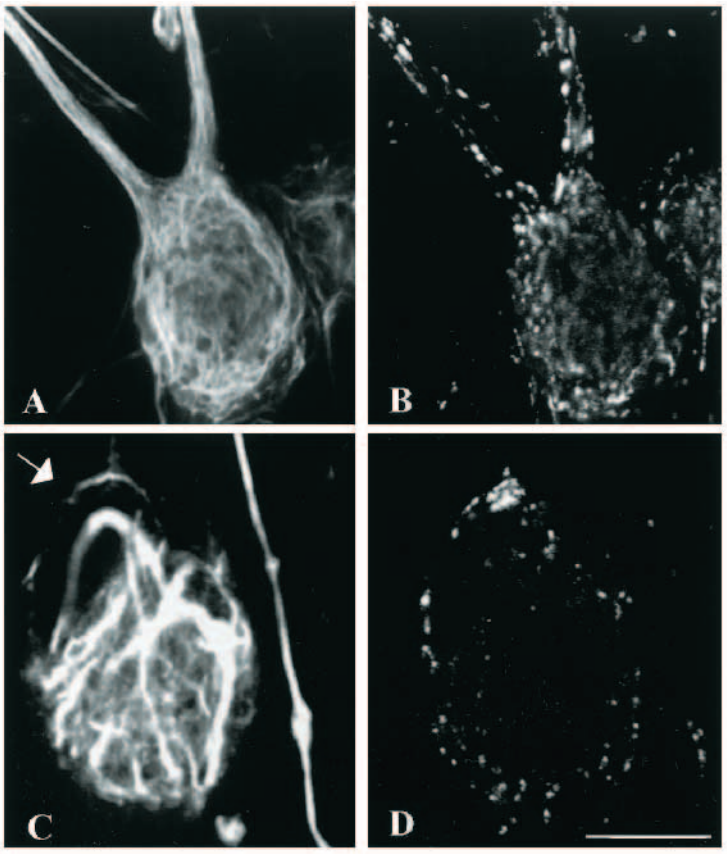

Fig. 5. The effects of NIF aggregation on mitochondrial localization. Mitochondria are distributed throughout the cell body and neurites in control cells (A,B). In cells containing NIF aggregates, mitochondria accumulate in the peripheral region of the cell bodies and adjacent to the entrances to neurites (C,D). Nuclear displacement is indicated by the arrow in C. Double label immunofluorescence with anti-NF-L (A,C) and anti-HSP60 (B,D). Bar, 10 μm.

cells containing NIF aggregates within 12-24 hours post-injection. During this time period, mitochondria accumulated in the peripheral region of cell bodies, especially in areas adjacent to entrances to neurites (Fig. 5C,D). In these same cells, very few mitochrondria could be detected along neurites relative to control cells (see Fig. 5A,B). As indicated above, another frequently observed change in subcellular morphology involved the displacement of the nucleus, which frequently appeared bulging from the cell surface (Fig. 5C,D, also see Fig. 3D).

Since both mitochondrial movements and Golgi complex organization are thought to be regulated by microtubules and their associated proteins (Pannese et al., 1986; Weissenfels et al., 1990; Kreis, 1990; Soltys and Gupta, 1992; Thyberg and Moskalewski, 1992; Letourneau and Wire, 1995), we sought to determine if microtubule patterns were altered upon the induction of the NIF aggregates. The results indicated that there were no obvious alterations in the patterns of microtubules coincident with the formation of NIF aggregates (data not shown).

Accumulation of NIF in the cell body is accompanied by a decrease in neurite caliber

Observations of cells induced to form NIF aggregates suggested that the thickness or caliber of neurites had decreased relative to control cells. To confirm this, we examined individual cells on locator coverslips using DIC optics before and after microinjection with 5 mg/ml of NF-H. Live neurons were observed on an inverted microscope and measurements were taken of neurite width in regions adjacent to the cell body. Three types of controls were used for these experiments; cells microinjected with injection buffer alone, with 1 mg/ml of NF-H, and uninjected cells. Measurements were made in all cases on live cells and following the last measurement, the coverslips were fixed and processed for indirect immunofluorescence. Of the cells injected with 1 or 5 mg/ml NF-H, only those which stained with anti-biotin were included in the statistical analysis. In the case of the injection of 5 mg/ml, only cells containing NIF aggregates were included.

Measurements of neurite width showed a decrease in the cells that contained NIF aggregates. Before microinjection, the average width was 3.1±0.7 μm and 24 hours after microinjection the average width was 2.6±0.5 μm. This difference is significant using a Student's *t*-test ($P<0.001$, $n=17$). Results from each of the remaining control groups revealed no statistical difference in neurite width before and 24 hours following treatment. Given that the microinjection of 1 mg/ml of NF-H did not alter neurite width ($P<0.30$, $n=13$), we can state that the addition of non-disruptive amounts of microinjected NF-H had no effect. Furthermore, the results of a one-way analysis of variance (ANOVA) revealed that the difference in neurite width before and after treatment was significant with respect to the treatment each group received ($F_{3,65}=5.78$, $P<0.005$). Analysis of the three control groups revealed no significant difference among the groups ($F_{2,49}=0.51$, $P<0.60$). Therefore, the decrease in neurite width observed in the group receiving 5 mg/ml of NF-H was a result of the microinjection of higher concentrations of NF-H and not the microinjection technique itself. The amount of decrease in the width of neurites in the high NF-H group was quite variable from cell to cell (21±15%)

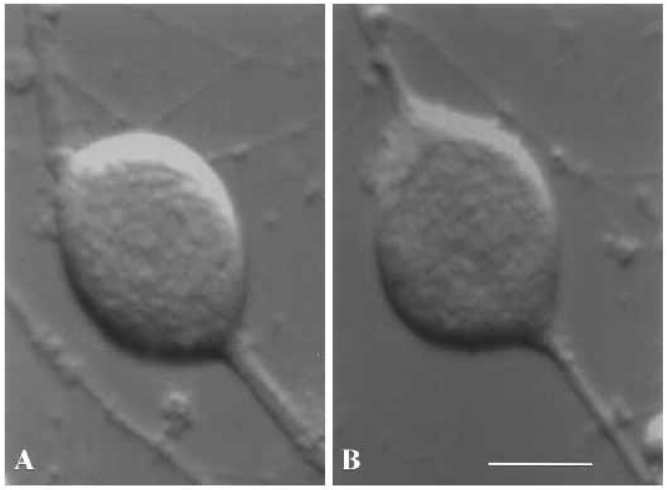

Fig. 6. Neurite width decreases following the induction of NIF aggregates. The same cell before (A) and 24 hours following (B) microinjection of 4-5 mg/ml NF-H. There is a measurable decrease of approximately 50% in the width of the proximal neurites of this cell as detected by differential interference microscopy. Bar, 10 μm.

and in some neurites was as high as 50%. This is probably due to the microinjection technique itself, as the amount of protein delivered to each cell is known to be variable (Lee, 1989; Minaschek et al., 1989). However, the overall impact of the formation of NIF aggregates is reflected by a significant decrease in the average widths of neurites (Fig. 6).

The NIF aggregates induced by NF-H become abnormally phosphorylated

NIF aggregates similar to those seen in microinjected cells have been reported to be one of the pathological hallmarks of motor neuron diseases such as ALS (Carpenter, 1968; Hirano et al., 1984). The latter are abnormally phosphorylated (Cork et al., 1986; Troncoso et al., 1986; Schmidt et al., 1987), as demonstrated by their staining with specific antibodies which recognize a highly phosphorylated form of NF-H, usually present only in axons (Manetto et al., 1988; Itoh et al., 1992). We used one such antibody to address the possibility that NIF accumulations induced within cell bodies at the higher concentrations of biotinylated NF-H might be abnormally phosphorylated. Injected cells were, therefore, stained with the phospho-NFH specific antibody RMO24 (Lee et al., 1987). Although NIF aggregates were detected within 3-6 hours post-injection, they did not react with this antibody as indicated by indirect immunofluorescence assays for over 24 hours (Fig. 7A,B). However, staining with the same antibody at 48 hours post-injection revealed NIF aggregates (Fig. 7C,D). After 72 hours, the NIF aggregates stained even more intensely with RMO24 (data not shown). Since spinal cord derived NFH is normally highly phosphorylated, we also carried out experiments with protein treated with alkaline phosphatase prior to microinjection. Following this treatment, the dephosphorylated NF-H no longer reacted with the phospho-NFH specific antibody as determined by immunoblotting (data not shown). The microinjection results with the dephosphorylated NF-H were identical with respect to staining post-injection with the RM024 antibody. This indicates that the induction of NIF aggregation occurs prior to phosphorylation and that the aggregates are not formed simply due to the introduction of a bolus of phosphorylated protein into the cell body.

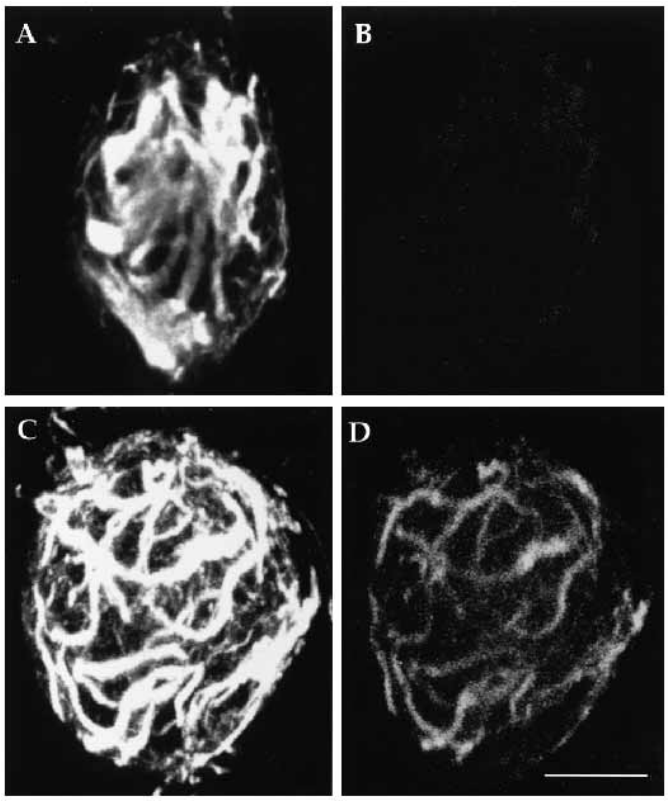

Fig. 7. A phosphorylation-state specific antibody recognizes NIF aggregates. Neurons were microinjected with 5 mg/ml NF-H to induce NIF aggregates and fixed for double label immunofluorescence at 24 hours (A,B) or 48 hours (C,D) post-injection. Staining with an antibody specific for a phosphorylated form of NF-H (RM024) revealed little or no immunoreactivity in NIF aggregate bearing neurons at 24 hours (A,B). However, RMO24 does recognize NIF aggregates in the microinjected cells by 48 hours post-injection (C,D). Double label immunofluorescence with anti-NF-L (A,C) and anti-phospho NFH (B,D). Bar, 10 μm.

DISCUSSION

The results of these investigations show that NFT proteins can become incorporated into endogenous NIF networks post-translationally and that NF-H can induce aggregates of NIF in a concentration dependent fashion. Following NIF aggregation, there are significant alterations in nerve cell architecture and organelle localization. Taken together, these observations support the dynamic nature of NIF and shed new light on their possible functions with respect to organelle localization and overall cell shape and size. Furthermore, the changes which are associated with NIF aggregation, are very similar to those seen in motor neuron diseases such as ALS. This provides us with an opportunity to begin to dissect not only the pathological consequences of NIF aggregation in single cells, but also the temporal sequence of cytological changes which represent hallmarks of motor neuron disease. Alterations in the relative amounts of NFT proteins can lead to NIF aggregation.

The results of the microinjection studies support previous work demonstrating that NFT proteins can become incorporated into endogenous NIF (also see Okabe et al., 1993; Takeda et al., 1994). In addition, our light microscopic results suggest that the pattern of incorporation of each of the NFT proteins is very similar, but that their rates of incorporation vary inversely according to their molecular masses. Therefore, NF-H is incorporated 1.5-2.0 times faster than NF-L. This is consistent with the data obtained from FRAP experiments which suggest that NF-H exchanges between assembled and disassembled states twice as fast as NF-L (Takeda et al., 1994). Further support for this observation comes from studies suggesting that NFH is the last of the triplet proteins to be expressed during development (Shaw and Weber, 1982; Willard and Simon, 1983; Pachter and Liem, 1984), and that it continues to exchange between soluble and filamentous pools after assembly into NIF (Hirokawa et al., 1984; Scott et al., 1985).

Most of the experiments in this study were focused on the consequences of altering the stoichiometric relationships of the NFT proteins to induce NIF aggregation. In this regard, several possible mechanisms can explain the affects of higher NF-H concentrations. For example, the long carboxy terminus of this protein may act to slow axonal transport due to steric drag on NIF (Shaw and Weber, 1982; Willard and Simon, 1983; Nixon and Sihag, 1991). Increased amounts of NF-H could also slow down transport of NIF causing them to accumulate and aggregate in the cell body. NF-H could also produce an excessive number of crossbridges between adjacent NIF and microtubules, thereby inhibiting their transport from cell bodies into axons. Such crossbridges are thought to be formed by the carboxy-tail regions of NF-H (Hirokawa, 1982; Geisler et al., 1983; Hirokawa et al., 1984; Hisanaga and Hirokawa, 1988, 1990; Nixon and Sihag, 1991; Miyasaka et al., 1993). Similar mechanisms have been proposed to explain the results obtained in the transgenic mice which overexpress human NF-H (Côté et al., 1993). Further support for such a mechanism is derived from the observation that neurotoxins such as IDPN and aluminum, known to depress slow axonal transport rates, also induce NIF aggregates in cell bodies (Griffin et al., 1978; Bizzi et al., 1984; Troncoso et al., 1985).

Since NIF are obligate heteropolymers in vivo (Ching and Liem, 1993; Lee et al., 1993), it should not be too surprising that alterations in the relative amounts of NFT subunits could lead to alterations in NIF organization. Estimates for the molar ratios amongst NF-L, NF-M, and NF-H subunits vary significantly in different types of neurons (e.g. Chiu et al., 1980; Schecket and Lasek, 1980). The published values range from 9:2:1 (Mori and Kurokawa, 1980) to 2:2:1 (Moon et al., 1981), indicating that normal NIF organization can be maintained over a range of subunit compositions perhaps reflecting the precise functions of NIF in different types of neurons. The data presented in this study strongly suggest that once the acceptable range of stoichiometric ratios for the NFT proteins is exceeded, there are serious functional aberrations and pathological consequences.

The relationship between nif aggregates and membranous organelle organization, distribution and transport

A phenomenon consistently observed within the cell bodies of NIF aggregate bearing neurons is a dispersed and fragmented Golgi complex. The fragmentation observed following NIF aggregation resembles the dispersion of the Golgi complex induced by colchicine and other microtubule depolymerizing agents (Robbins and Gonatas, 1964; Turner and Tartakoff, 1989). However, no obvious organizational changes in microtubules can be detected in the injected neurons containing NIF aggregates. These observations suggest that NIF also play a role in the organization of the Golgi complex. Interestingly, it has been reported by several laboratories that the Golgi complex is fragmented and dispersed in diseased NIF aggregate containing neurons derived from ALS patient tissues (Mourelatos et al., 1990, 1993, 1994; Gonatas et al., 1992; Tascos et al., 1995).

The accumulation of mitochondria in the most proximal region of neurites may be due to the general impairment of the axonal transport system that is related to the large NIF aggregates formed in response to elevated levels of NF-H. Studies on diseased neurons isolated from ALS patients have revealed altered transport speeds and organelle (e.g. mitochondrion) traffic density relative to control neurons (Breuer et al., 1987). It has been suggested that this decreased transport of mitochondria could result in the distal atrophy observed in ALS diseased axons (Bowling et al., 1993). This result is supported by studies of other cell types which also show a significant relationship between the subcellular distribution of mitochondria and vimentin containing intermediate filaments (see Wang and Goldman, 1978; Mose-Larsen et al., 1983; Welsh and Suhan, 1985). Furthermore, transgenic mice overexpressing NF-H exhibit defects in the axonal transport of not only mitochondria, but also tubulin, actin and the NFT proteins (Collard et al., 1995).

The relationship between nif and axon caliber

Our results also link NIF aggregate formation with a decrease in neurite caliber. This morphological change is most likely related to the impaired transport of NIF from the cell body into neurites. In support of this possibility, extensive morphometric analyses have demonstrated a positive correlation between the number of NIF and axon caliber (Friede and Samorajski, 1970; Weiss and Mayr, 1971). In the case of the Quiver mutant quail, no NIF are found and axon diameter is greatly decreased (Ohara et al., 1993; Yamasaki et al., 1992). In contrast, it has been shown that increasing the number of NIF by overexpressing NF-L, does not lead to an increase in axon caliber in transgenic mice (Monteiro et al., 1990). This latter result may, in part be explained by a relative decrease in the amount of NF-H in these mice which in turn could lead to a reduction in inter-NIF spacing, thereby maintaining normal axon caliber.

NIF aggregation precedes abnormal phosphorylation within the cell body

The observation that NIF aggregates induced by the microinjection method react with the phosphorylation-state dependent antibody, RMO24 (Lee et al., 1987), also reflects the changes seen in motor neuron diseases such as ALS. This antibody recognizes a highly phosphorylated form of NF-H, normally present in axons but not in cell bodies. It also recognizes NIF aggregates in postmortem preparations of ALS motor neurons (Lee et al., 1987; Schmidt et al., 1987). One explanation for this observation lies in the possibility that NIF are normally phosphorylated just prior to transport from the cell body into

axons. Therefore, any impairment of the transport machinery could lead subsequently to an abnormal accumulation of phosphorylated NIF. If this scenario is true, then the NIF aggregates induced by the microinjection method used in this study should react with RMO24 as soon as they are formed. However, the results obtained from cells injected with the higher concentrations of NF-H demonstrate that the NIF aggregates form long before abnormal phosphorylation can be detected. It appears, therefore, that the initiation of NIF aggregation does not require the presence of abnormally phosphorylated NF-H.

In summary, we have presented evidence that cultured neurons can incorporate NFT proteins into endogenous NIF at the post-translational level. This lends further support to the notion that NIF are dynamic structures in vivo. Furthermore, the organization of NIF networks can be altered by raising the concentration of NF-H microinjected into these cells. The resulting accumulation of NIF in the cell body triggers a cascade of morphological and physiological changes which not only shed new light on the normal functions of NIF, but also help to determine their roles in neuropathological processes.

The authors thank Rob Mihalik and Satya Khuon for technical assistance and Laura Davis for helping us with manuscript preparation. This work was supported by the Les Turner ALS Foundation and a pre-doctoral fellowship (Karen Straube-West) from the NIMH.

REFERENCES

Aebi, U., Haner, M., Troncoso, J., Eichner, R. and Engel, A. (1988). Unifying principles in intermediate filament (IF) structure and assembly. *Protoplasma* **145**, 73-81.

Angelides, K. J., Smith, K. E. and Takeda, M. (1989). Assembly and exchange of intermediate filament proteins of neurons: neurofilaments are dynamic structures. *J. Cell Biol.* **108**, 1495-1506.

Arakawa, O.-M. and Narahashi, T. (1992). Chloride current induced by alcohols in rat dorsal root ganglion neurons. *Brain Res.* **578**, 275-281.

Balin, B. J. and Lee, V. M.-Y. (1991). Individual neurofilament subunits reassembled in vitro exhibit unique biochemical, morphological and immunological properties. *Brain Res.* **556**, 196-208.

Bennett, G. S., Tapscott, S. J., Kleinbart, F. A., Antin, P. B. and Holtzer, H. (1981). Different proteins associated with 10-nanometer filaments in cultured chick neurons and non-neuronal cells. *Science* **212**, 567-569.

Bennett, G. S., Tapscott, S. J., DiLullo, C. and Holtzer, H. (1984). Differential binding of antibodies against the neurofilament triplet proteins in different avian neurons. *Brain Res.* **304**, 291-302.

Bizzi, A., Crane, R. C., Autilio-Gambetti, L. and Gambetti, P. (1984). Aluminum effect on slow axonal transport: a novel impairment of neurofilament transport. *J. Neurosci.* **4**, 722-731.

Bowling, A. C., Schulz, J. S., Brown, R. H. and Beal, M. F. (1993). Superoxide dismutase activity, oxidative damage, and mitochondrial energy metabolism in familial and sporatic amyotrophic lateral sclerosis. *J. Neurochem.* **61**, 2322-2325.

Bradford, M. M. (1976). A rapid and sensitive method for the quantitation of microgram quantities of protein utilizing the principle of protein-dye binding. *Anal. Biochem.* **72**, 248-254.

Breuer, A. C., Lynn, M. P., Atkinson, M. B., Chou, S. M., Wilbourn, A. J., Marks, K. E., Culver, J. E. and Fleegler, E. J. (1987). Fast axonal transport in amyotrophic lateral sclerosis: an intra-axonal organelle traffic analysis. *Neurology* **37**, 738-748.

Carden, M. J., Schlaepfer, W. W. and Lee, V. M.-Y. (1985). The structure, biochemical properties, and immunogenicity of neurofilament peripheral regions are determined by phosphorylation state. *J. Biol. Chem.* **260**, 9805-9817.

Carpenter, S. (1968). Proximal axonal enlargement in motor neuron disease. *Neurology* **18**, 841-851.

Ching, G. Y. and Liem, R. K. H. (1993). Assembly of Type IV neuronal intermediate filaments in non-neuronal cells in the absence of pre-existing cytoplasmic intermediate filaments. *J. Cell Biol*. **122**, 1323-1335.

Chiu, F.-C., Korey, B. and Norton, W. T. (1980). Intermediate filaments from bovine, rat and human CNS: mapping analysis of major proteins. *J. Neurochem.* **34**, 1149-1159.

Collard, J.-F., Côté, F. and Julien, J.-P. (1995). Defective axonal transport in a transgenic mouse model of amyotrophic lateral sclerosis. *Nature* **375**, 61-64.

Cork, L. C., Sternberger, N. H., Sternberger, L. A., Casanova, M. F., Strubl, R. G. and Price, D. L. (1986). Phosphorylated neurofilament antigens in neurofibrillary tangles in Alzheimer's disease. *J. Neuropath. Exp. Neurol.* **45**, 56-64.

Côté, F., Collard, J.-F. and Julien, J.-P. (1993). Progressive neuronopathy in transgenic mice expressing the neurofilament heavy gene: a mouse model of amyotrophic lateral sclerosis. *Cell* **73**, 35-46.

deWaegh, S. M., Lee, V. M.-Y. and Brady, S. T. (1992). Local modulation of neurofilament phosphorylation, axonal caliber, and slow axonal transport by myelinating Schwann cells. *Cell* **68**, 451-463.

Friede, R. L. and Samorajski, T. (1970). Axonal caliber related to neurofilaments and microtubules in sciatic nerve fibres of rats and mice. *Anat. Rec.* **167**, 379-388.

Gardner, E. E., Dahl, D. and Bignami, A. (1984). Formation of 10nm filaments from the 150K-Dalton neurofilament protein in vitro. *J. Neurosci. Res.* **11**, 145-155.

Gasser, H. S. and Grundfest, H. (1939). Axon diameters in relation to spike dimensions and the conduction velocity in mammalian A fibers. *Am. J. Physiol.* **127**, 393-414.

Geisler, N. and Weber, K. (1981). Self-assembly in vitro of the 68,000 molecular weight component of the mammalian neurofilament triplet proteins into intermediate-sized filaments. *J. Mol. Biol.* **151**, 565-571.

Geisler, N., Kaufmann, E., Fischer, S., Plessmann, U. and Weber, K. (1983). Neurofilament architecture combines structural principles of intermediate filaments with carboxy-terminal extensions increasing in size between triplet proteins. *EMBO J.* **2**, 1295-1302.

Gonatas, N. K., Stieber, A., Mourelatos, Z., Chen, Y., Gonatas, J. O., Appel, S. H., Hays, A. P., Hickey, W. F. and Hauw, J. J. (1992). Fragmentation of the Golgi apparatus of motor neurons in amyotrophic lateral sclerosis. *Am. J. Pathol.* **140**, 731-737.

Griffin, J. W., Hoffman, P. N., Clark, A. W., Carroll, P. T. and Price, D. L. (1978). Slow axonal transport of neurofilament proteins: impairment of beta,beta′-iminodipropionitrile adminstration. *Science* **202**, 633-635.

Hamburger, V. and Hamilton, H. L. (1951). A series of normal stages in the development of the chick embryo. *J. Morphol.* **88**, 49-92.

Henneman, E., Somjen, G. and Carpenter, D. O. (1965). Excitability and inhibitability of motoneurons of different sizes. *J. Neurophysiol.* **28**, 599-619.

Hirano, A., Donnenfeld, H., Sasaki, S. and Nakano, I. (1984). Fine structured observations of neurofilamentous changes in amyotrophic lateral sclerosis. *J. Neuropathol. Exp. Neurol.* **43**, 461-470.

Hirokawa, N. (1982). The crosslinker system between neurofilaments, microtubules and membranous organelles in frog axons revealed by quick-freeze, freeze-fracture, deep-etching method. *J. Cell Biol*. **94**, 129-142.

Hirokawa, N., Glicksman, M. A. and Willard, M. (1984). Organization of mammalian neurofilament polypeptides within the neuronal cytoskeleton. *J. Cell Biol.* **98**, 1523-1536.

Hisanaga, S. and Hirokawa, N. (1988). Structure of the peripheral domains of neurofilaments revealed by low angle rotary shadowing. *J. Mol. Biol.* **202**, 297-305.

Hisanaga, S. and Hirokawa, N. (1990). Dephosphorylation-induced interactions of neurofilaments with microtubules. *J. Biochem.* **265**, 21852-21858.

Hoffman, P. N. and Lasek, R. J. (1975). The slow component of axonal transport: Identification of the major structural polypeptides of the axon and their generality among mammalian neurons. *J. Cell Biol.* **66**, 351-366.

Hoffman, P. N., Griffin, J. W. and Price, D. L. (1984). Control of axonal caliber by neurofilament transport. *J. Cell Biol.* **99**, 705-714.

Hoffman, P. N., Thompson, G. W., Griffin, J. and Price, D. L. (1985). Changes in neurofilament transport coincide temporally with alterations in the caliber of axons in regenerating motor fibers. *J. Cell Biol.* **101**, 1332-1340.

Itoh, T., Sobue, G., Ken, E., Mitsuma, T., Takahashi, A. and Trojanowski. J. Q. (1992). Phosphorylated high molecular weight neurofilament protein in the peripheral motor, sensory and sympathetic neuronal perikarya: system-dependent normal variations and changes in amyotrophic lateral sclerosis and multiple system atrophy. *Acta Neuropathol.* **83**, 240-245.

Kreis, T. E. (1990). Role of microtubules in the organization of the Golgi apparatus. *Cell Motil. Cytoskel.* **15**, 67-70.

Laemmli, U. K. (1970). Cleavage of structural proteins during the assembly of the head of the bacteriophage T4. *Nature* **227**, 680-685.

Lee, G. M. (1989). Measurement of volume injected into individual cells by quantitative fluorescence microscopy. *J. Cell Sci.* **94**, 443-447.

Lee, M. K., Xu, Z., Wong, P. C. and Cleveland, D. W. (1993). Neurofilaments are obligate heteropolymers in vivo. *J. Cell Biol.* **122**, 1337-1350.

Lee, M. K., Marszalek, J. R. and Cleveland, D. W. (1994). A mutant neurofilament subunit causes massive, selective motor neuron death: implications for pathogenesis of human motor neuron disease. *Neuron* **13**, 975-988.

Lee, V. M.-Y., Carden, M. J., Schlaepfer, W. W. and Trojanowski, J. Q. (1987). Monoclonal antibodies distinguish several differentially phosphorylated states of the two largest rat neurofilament subunits (NF-H and NF-M) and demonstrate their existence in the normal nervous system of adult rats. *J. Neurosci.* **7**, 3474-3488.

Letourneau, P. C. and Wire, J. P. (1995). Three dimensional organization of stable microtubules and the Golgi apparatus in the somata of developing chick sensory neurons. *J. Neurocytol.* **24**, 207-223.

Liem, R. K. H., Yen, S.-H., Solomon, G. D. and Shelanski, M. L. (1978). Intermediate filaments in nervous tissue. *J. Cell Biol.* **79**, 637-645.

Liem, R. K. H. and Hutchinson, C. (1982). Purification of individual components of the neurofilament triplet: filament assembly from the 70,000 dalton subunit. *Biochemistry* **21**, 3221-3226.

Manetto, V., Sternberger, N. H., Perry, G., Sternberger, L. A. and Gambetti, P. (1988). Phosphorylation of neurofilaments is altered in amyotrophic lateral sclerosis. *J. Neuropath. Exp. Neurol.* **47**, 642-653.

Miller, R. K., Khuon, S. and Goldman, R. D. (1993). Dynamics of keratin assembly: exogenous Type I keratin rapidly associates with Type II keratin in vivo. *J. Cell Biol.* **122**, 123-135.

Minaschek, G., Beriter-Hahn, J. and Bertholdt, G. (1989). Quantitation of the volume of liquid injected into cells by means of pressure. *Exp. Cell Res.* **183**, 434-432.

Miyasaka, H., Okabe, S., Ishiguro, K., Uchida, T. and Hirokawa, N. (1993). Interaction of the tail domain of high molecular weight subunits of neurofilaments with the COOH-terminal region of tubulin and its regulation by tau protein kinase II. *J. Biol. Chem.* **268**, 22695-22702.

Monteiro, M. J., Hoffman, P. N., Gearhart, J. D. and Cleveland, D. W. (1990). Expression of NF-L in both neuronal and non-neuronal cells of transgenic mice: increased neurofilament density in axons without affecting caliber. *J. Cell Biol.* **111**, 1543-1557.

Moon, H. M., Wisniewski, T., Merz, P., DeMartin, J. and Wisniewski, H. M. (1981). Partial purification of subunits from bovine brains and studies on neurofilament assembly. *J. Cell Biol.* **89**, 560-567.

Mori, H. and Kurokawa, M. (1980). Morphological and biochemical characterization of neurofilaments isolated from rat peripheral nerve. *Biochem. Res.* **1**, 24-30.

Mose-Larsen, P., Bravo, R., Fey, S. Y., Small, J. V. and Celis, J. E. (1983). Putative association of mitochondria with a subpopulation of intermediate-sized filaments in cultured human skin fibroblasts. *Cell* **31**, 681-692.

Mourelatos, Z., Adler, H., Hirano, A., Donnenfeld, H. D., Gonatas, J. O. and Gonatas, N. K. (1990). Fragmentation of the Golgi apparatus of motor neurons in amyotrophic lateral sclerosis revealed by organelle-specific antibodies. *Proc. Nat. Acad. Sci. USA* **87**, 4393-4395.

Mourelatos, Z., Yachnis, A., Rorke, L., Mikol, J. and Gonatas, N. K. (1993). The Golgi apparatus of motor neurons in amyotrophic lateral sclerosis. *Ann. Neurol.* **33**, 608-615.

Mourelatos, A., Hirano, A., Rosenquist, A. C. and Gonatas, N. K. (1994). Fragmentation of the Golgi apparatus of motor neurons in amyotrophic lateral sclerosis (ALS). *Am. J. Pathol.* **144**, 1288-1300.

Nakagawa, T., Chen, J., Zhang, Z., Kanai, Y. and Hirokawa, N. (1995). Two distinct functions of the carboxyl-tail domain of NF-M upon neurofilament assembly: cross bridge formation and longitudinal elongation of filaments. *J. Cell Biol.* **129**, 411-429.

Nixon, R. A. and Sihag, R. K. (1991). Neurofilament phosphorylation: a new look at regulation and function. *Trends Neurosci.* **14**, 501-506.

Nixon, R. A. and Shea, T. B. (1992). Dynamics of neuronal intermediate filaments: a developmental perspective. *Cell Motil. Cytoskel.* **22**, 81-91.

Nixon, R. A. (1993). The regulation of protein dynamics by phosphorylation: clues to neurofibrillary pathobiology. *Brain Pathol.* **3**, 29-38.

Ohara, O., Gahra, Y., Miyake, T., Teraoka, H. and Kitamura, T. (1993). Neurofilament deficiency in quail caused by nonsense mutation in neurofilament-L gene. *J. Cell Biol.* **121**, 387-395.

Okabe, S., Miyasaka, H. and Hirokawa, N. (1993). Dynamics of the neuronal intermediate filaments. *J. Cell Biol.* **121**, 375-386.

Pachter, J. S. and Liem, R. K. H. (1984). The differential appearance of neurofilament triplet polypeptides in the developing rat optic nerve. *Dev. Biol.* **103**, 200-210.

Pannese, E., Procacci, P., Ledda, M., Arcidiacono, G., Frattola, D. and Rigamonti, L. (1986). Associations between microtubules and mitochondria in myelinated axons of *Lacerta muralis*. A quantitative analysis. *Cell Tissue Res.* **245**, 1-8.

Robbins, E. and Gonatas, N. K. (1964). Histochemical and ultrastructural studies on HeLa cell cultures exposed to spindle inhibitors with special reference to the interphase cell. *J. Histochem. Cytochem.* **12**, 704-711.

Schecket, G. and Lasek, R. J. (1980). Preparation of neurofilament protein from guinea pig peripheral nerve and spinal cord. *J. Neurochem.* **35**, 1335-1344.

Schmidt, M. L., Carden, M. J., Lee, V. M.-Y. and Trojanowski, J. Q. (1987). Phosphate depedent and independent neurofilament epitopes in the axonal swellings of patients with motor neuron disease and controls. *Lab. Invest.* **56**, 282-294.

Scott, D., Smith, K. E., O'Brien, B. and Angelides, K. J. (1985). Characterization of mammalian neurofilament triplet proteins: subunit stoichiometry and morphology of nature and reconstituted filaments. *J. Biol. Chem.* **260**, 10736-10797.

Shaw, G. and Weber, K. (1982). Differential expression of neurofilament triplet proteins in brain development. *Nature* **298**, 276-299.

Shaw, G. (1991). Neurofilament proteins. In *The Neuronal Cytoskeleton* (ed. R. D. Burgoyne), pp. 75-93. Wiley-Liss, NY.

Soltys, B. J. and Gupta, R. S. (1992). Interrelationships of endoplasmic reticulum, mitochondria, intermediate filaments, and microtubules - a quadruple fluorescence labeling study. *Biochem. Cell Biol.* **70**, 1174-1186.

Steinert, P. M. and Roop, D. R. (1988). The molecular and cellular biology of intermediate filaments. *Annu. Rev. Biochem.* **57**, 593-625.

Sternberger, L. A. and Sternberger, N. (1983). Monoclonal antibodies distinguish phosphorylated and non-phosphorylated forms of neurofilaments *in situ*. *Proc. Nat. Acad. Sci. USA* **80**, 6126-6130.

Takeda, S., Okabe, S., Funakoshi, T. and Hirokawa, N. (1994). Differential dynamics of neurofilament-H proteins and neurofilament-L protein in neurons. *J. Cell Biol.* **127**, 173-185.

Tascos, N., Mourelatos, Z. and Gonatas, N. K. (1995). On the significance and reproducibility of the fragmentation of the Golgi apparatus of motor neurons in human spinal cords. *J. Neuropath. Exp. Neurol.* **54**, 331-338.

Thyberg, J. and Moskalewski, S. (1992). Disorganization of the Golgi complex and the cytoplasmic microtubule system in CHO cells exposed to okadaic acid. *J. Cell Sci.* **103**, 1167-1175.

Towbin, J., Staehelin, T. and Gordon, J. (1979). Electrophoretic transfer of proteins from polyacrylamide gels to nitrocellulose sheets: procedure and some applications. *Proc. Nat. Acad. Sci. USA* **76**, 4350-4354.

Troncoso, J. C., Hoffman, P. N., Griffin, J. W., Hess-Kozlow, K. M. and Price, D. (1985). Aluminum intoxication: a disorder of neurofilament transport in motor neurons. *Brain Res.* **342**, 172-175.

Troncoso, J. C., Sternberger, N. H., Sternberger, L. A., Hoffman, P. N. and Price, D. L. (1986). Immunocytochemical studies of neurofilament antigens in the neurofibrillary pathology induced by aluminum. *Brain Res.* **364**, 295-300.

Turner, J. R. and Tartakoff, A. M. (1990). The response of the Golgi complex to microtubule alterations: the roles of metabolic energy and membrane traffic in Golgi complex organization. *J. Cell Biol.* **109**, 2081-2088.

Vickers, J. C., Morrison, J. H., Friedrich, V. L. Jr, Elder, G. A., Perl, D. P., Katz, R. N. and Lazzarini, R. A. (1994). Age-associated and cell-type-specific neurofibrillary pathology in transgenic mice expressing the human midsized neurofilament subunit. *J. Neurosci.* **14**, 5603-5612.

Vikstrom, K. L., Borisy, G. G. and Goldman, R. D. (1989). Dynamic aspects of intermediate filament networks in BHK-21 cells. *Proc. Nat. Acad. Sci. USA* **86**, 549-553.

Vikstrom, K. L., Miller, R. K. and Goldman, R. D. (1990). Methods for analyzing the dynamic properties of intermediate filaments. *Meth. Enzymol.* **196**, 506-525.

Vikstrom, K. L., Lim, S.-S., Goldman, R. D. and Borisy, G. G. (1992). Steady state dynamics of intermediate filament networks. *J. Cell Biol.* **118**, 121-129.

Voyvodic, J. T. (1989). Target size regulates calibre and myelination of sympathetic axons. *Nature* **342**, 430-433.

Wang, E. and Goldman, R. D. (1978). Functions of cytoplasmic fibers in

intracellular organelle movements in BHK-21 cells. *J. Cell Biol*. **79**, 708-726.

Weiss, P. A. and Mayr, R. (1971). Organelles of neuroplasmic ('axonal') flow: neurofilaments. *Proc. Nat. Acad. Sci. USA* **68**, 846-850.

Weissenfels, N., Wachtmann, D. and Stockem, W. (1990). The role of microtubules for the movements of mitochondria in pinacocytes of fresh-water sponges. *Eur. J. Cell Biol*. **52**, 310-314.

Welsh, W. J. and Sukan, J. B. (1985). Morphological study of the mammalian stress response: characterization of changes in cytoplasmic organelles, cytoskeleton, and nucleoli and appearance of intranuclear actin filaments in rat fibroblasts after heat shock treatment. *J. Cell Biol*. **101**, 1198-1211.

Willard, M. and Simon, C. (1983). Modulation of neurofilament transport during the development of rabbit retinal ganglion cells. *Cell* **35**, 551-559.

Xu, Z., Cork, L. C., Griffin, J. W. and Cleveland, D. W. (1993). Increased expression of neurofilament subuit NF-L produces morphological alterations that resemble the pathology of human motor neuron disease. *Cell* **73**, 23-33.

Yamasaki, H., Bennett, G., Itakura, C. and Mizutani, M. (1992). Defective expression of neurofilament protein subunits in hereditary hypotrophic axonopathy of quail. *Lab. Invest*. **66**, 734-743.

Yang, H. Y., Lieska, N., Goldman, A. E. and Goldman, R. D. (1985). A 300,000-mol-wt intermediate filament associated protein in baby hamster kidney. *J. Cell Biol*. **100**, 620-631.

Zackroff, R. V., Idler, W. W., Steinert, P. M. and Goldman, R. D. (1982). In vitro reconstitution of intermediate filaments from mammalian neurofilament triplet polypeptides. *Proc. Nat. Acad. Sci. USA* **79**, 754-757.

(Received 25 March 1996 - Accepted 28 May 1996)